Flexural and Shear Behavior of 3D Printed Reinforced Concrete Beams: An Experimental Study

Budiman, F.[1], Halim, A.[1], Chandra, J.[1*], and Pudjisuryadi, P.[1]

Abstract: 3D Concrete Printing (3DCP) provides many advantages for construction industry especially on productivity, waste, labor, and environment. Many researches have been conducted on the material development for 3DCP. However, there are not many researches which study the structural behavior of 3DCP. This experimental research aims to analyze flexural and shear behavior of 3D printed reinforced concrete beams. Five longitudinal reinforcement ratios were used to analyze crack patterns, failure mode, ductility, and capacity of those beams. The experimental results were then compared with analytical results by using ACI design code. The results show that higher longitudinal reinforcement ratio yields higher flexural and shear capacity of 3DCP beams. Due to layer-by-layer printing process, 3DCP beams are prone to local failure of filaments. Placement of longitudinal reinforcement might initiate macroscopic voids which could cause slippage and sudden drop on the capacity. Furthermore, ACI code underestimates the capacity of 3DCP beams failing in shear by some margins.

Keywords: 3D printed reinforced concrete beams; flexural behavior; shear behavior; experimental study; design code; longitudinal reinforcement ratio.

Introduction

Additive manufacturing or 3D printing technology is an automation procedure which produces a component from a digital model [1]. This technology has been widely used in many scientific fields but its usage in Civil Engineering is still in the research phase. Concrete is one of construction materials that can be made using 3D printing technology (3D printed concrete) which is considered as new technology in construction. Utilization of 3D printed concrete will reduce material waste, labor cost, and construction time [2].

Concrete is a material that is weak against tension stress with brittle mode of failure. Therefore, tension failure must be avoided. This material characteristic is also found on the 3D printed concrete [3] with anisotropic behavior [4]. Anisotropic behavior is caused by the production process of 3D printed concrete that prints concrete layer-by-layer and thus it makes the density and bond between layers (interlayer bonding) significantly lower [5]. In order to withstand tension stress, concrete is usually reinforced by steel reinforcing bar.

When steel reinforcing bar is used, tension stress will be resisted by the steel reinforcing bar while compression stress is resisted by the concrete.

Many studies have studied the hardened properties of 3D printed concrete. From the studies, it is concluded that anisotropic behavior is apparent on flexural, shear, and compression capacity of 3D printed concrete [3,4,6,7]. It is also concluded that interlayer bonding is affected by the humidity between concrete layers which is usually lower when printing time gap between layer is longer [3] and is influenced by bleeding of the concrete [6]. Loading at the 3D printed concrete layer will yield higher shear strength than loading at the 3D printed concrete interlayer [7]. Height of extruder nozzle does not affect the characteristics of 3D printed concrete and a proper curing will increase the hardened properties of 3D printed concrete [3].

Numerous studies have also been conducted on the effect and behavior of reinforcement on 3D printed concrete [8-13]. From the pull-out test done by Baz et al. [8] and Ding et al. [9], it can be concluded that bond strength between steel and 3D printed concrete is higher when steel bar is placed parallel with the 3D printed concrete layer and is lower when the bar is placed perpendicular to the 3D printed concrete layer because of macroscopic void. Sun et al. [10] studied the shear strength of 3D printed concrete beams by direct shear test using flexible and rigid reinforcement and inferred that flexible and rigid reinforcement increased the shear strength of 3D printed

[1] Department of Civil Engineering, Faculty of Civil Engineering and Planning, Petra Christian University, Jl. Siwalankerto 121-131, Surabaya 60236, INDONESIA
*Corresponding author; Email: chandra.jimmy@petra.ac.id

concrete from dowel action mechanism (rigid and flexible) and bond between steel and concrete (rigid). Al-Chaar et al. [11] used mesh and steel bar to reinforce 3D printed concrete truss beams and concluded that higher ratio of steel reinforcement yielded higher capacity of 3D printed concrete truss beams. Asprone et al. [12] utilized external steel rod reinforcement on 3D printed concrete truss beams and showed that failure mostly occurred on the joint (nodal zone) of 3D printed concrete truss beams. Gebhard et al. [13] analyzed the use of prestressing strand and fiber for reinforcing 3D printed concrete beams and showed that fiber and prestressing strand increased the flexural capacity and changed the mode of failure from shear to flexure. However, few studies have been conducted to study the effect of conventionally placed steel bar on the behavior of 3D printed concrete beams subjected to flexural and shear stresses.

This research investigates the structural behavior of 3D printed concrete beams with variation of longitudinal reinforcement. Experimental study is conducted by producing both conventionally casted and 3D printed concrete beams for a better comparison between these two methods of concrete production. The flexural and shear capacities of both conventionally casted and 3D printed concrete beams are then compared with the capacities acquired from building code [14]. It is expected that this research will further increase the understanding about flexural and shear behavior of 3D printed concrete beams.

Building Code Provisions

ACI 318-14 Provisions

According to ACI 318-14, Chapter 22 [14], the nominal shear strength (V_n) of non-prestressed concrete member without axial load can be taken as the lowest value calculated from equations tabulated on Table 1.

Table 1. Nominal Shear Strength (V_n) Equations.

V_n	
$\left[0.16\lambda\sqrt{f_c'} + 17\rho_w \dfrac{V_u d}{M_u}\right] b_w d$	(1)
$\left[0.16\lambda\sqrt{f_c'} + 17\rho_w\right] b_w d$	(2)
$0.29\lambda\sqrt{f_c'}b_w d$	(3)

where V_n is nominal shear strength, in N; λ is modification factor reflecting the reduced mechanical properties for lightweight concrete; f_c' is concrete compressive strength, in MPa; ρ_w is ratio of longitudinal reinforcement, V_u is maximum shear force, in N; M_u is maximum moment, in Nmm; b_w is width of concrete member, in mm; and d is effective height of concrete member, in mm.

The calculation of moment nominal capacity (M_n) of non-prestressed concrete member without axial load is taken from Chapter 22 of ACI 318-14 [14]. The equation is:

$$M_n = A_s f_y \left(d - \frac{\beta_1 c}{2}\right) \tag{4}$$

where M_n is moment nominal capacity, in Nmm; A_s is area of longitudinal reinforcement, in mm^2; f_y is yield strength of longitudinal reinforcement, in MPa; d is effective height of concrete member, in mm; β_1 is modification factor to calculate equivalent concrete stress block distribution; c is neutral axis depth of concrete member, in mm.

Laboratory Experiment

Specimen Details

In order to fully understand the effect of longitudinal reinforcement ratio on flexural and shear behavior of 3D printed concrete beams, five longitudinal reinforcement ratios were used (0%, 0.37% 0.73%, 1.05%, 1.32%) as shown in Figure 1. The dimension of the specimens is 550 x 100 x 100 mm. Considering the possibility of slippage between reinforcement and concrete, the longitudinal reinforcements were welded to a steel plate (150 x 100 x 6 mm) after printing and then grouted to the concrete beams. Therefore, the final dimension of the specimens is 650 x 100 x 100 mm for specimens with more than 0% reinforcing ratio whereas for specimen with 0% reinforcing ratio, the dimension is 550 x 100 x 100 mm, as visualized in Figure 2.

Materials

The mix proportions of the 3D printed concrete are listed on Table 2. In this study, portland composite cement (PCC) (PT. Semen Indonesia Tbk) was used as the cementitious material. The aggregate used in the mix was fine silica sand with grain size smaller than 0.8 mm. Superplasticizer (SP) (Sika® Viscocrete 1003) and Viscosity Modifying Admixture (VMA) (Sika® Stabilizer-4 R) were used to improve flowability and reduce bleeding of the fresh concrete. Accelerator (SikaSet® Accelerator) was used to increase early strength of the concrete and to reduce shrinkage. Very fine (Mesh 2000) calcium carbonate ($CaCO_3$) (PT. Dwi Selo Giri Mas) was used to enhance the cohesiveness of the mixture. Cement grout (SikaGrout® 215) was used as the grouting material. The reinforcing materials were taken from wiremesh which then cut to conventional steel reinforcing bar. The reinforcing material properties and stress–strain relationships are shown in Table 3 and Figure 3, respectively.
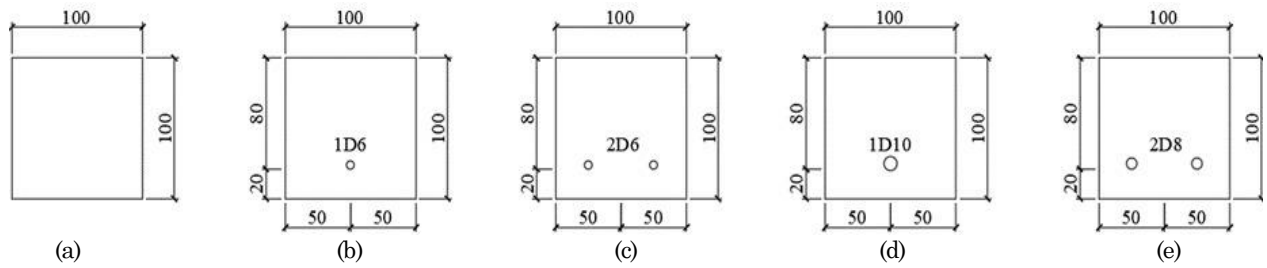
Figure 1. Specimen Reinforcement Detail of Beams with (a) 0%, (b) 0.37%, (c) 0.73%, (d) 1.05%, and (e) 1.32% Longitudinal Reinforcement Ratio
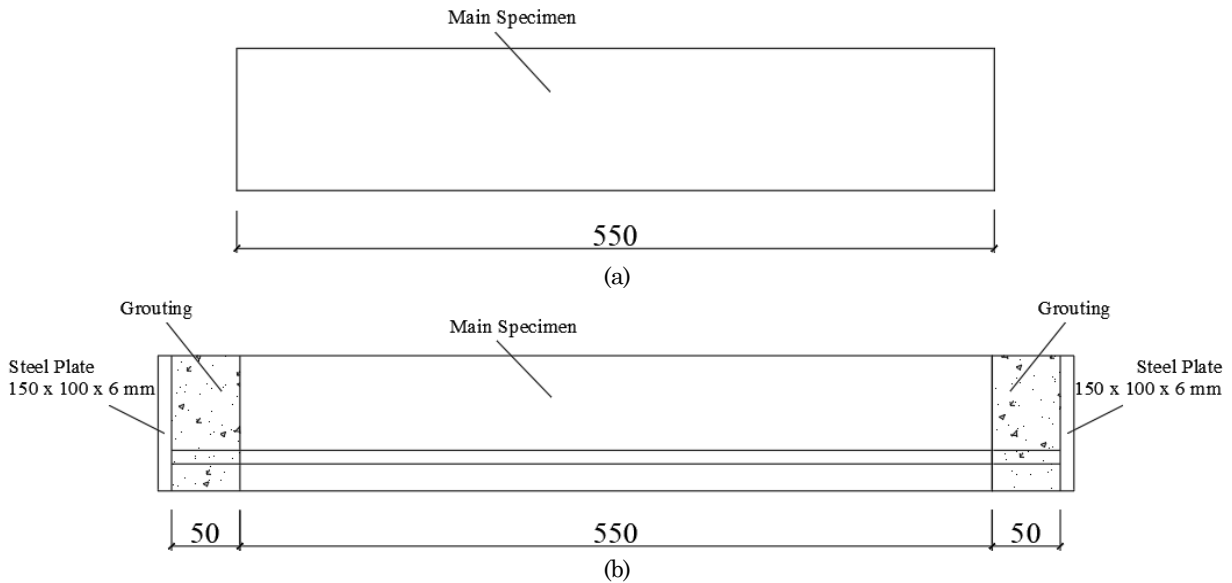
Figure 2. Specimen Dimensions (in mm); (a) Beam with no Reinforcement and (b) Beams with Longitudinal Reinforcement
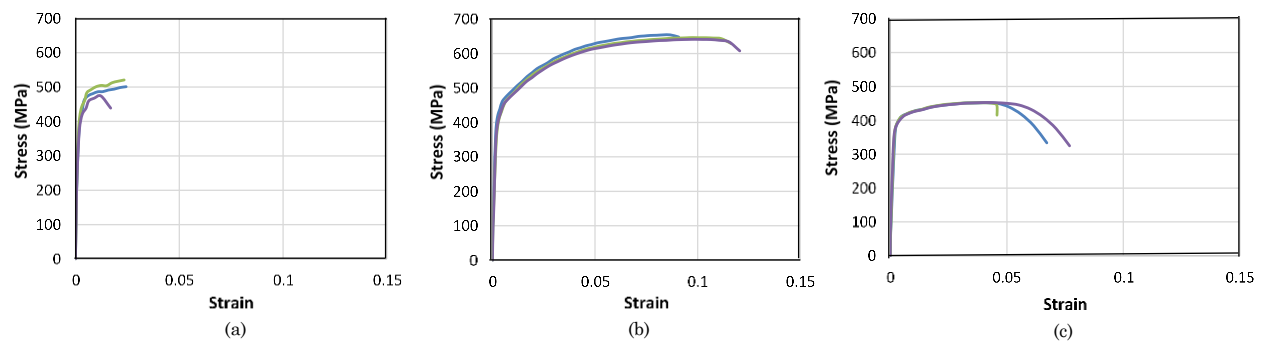
Table 2. Mixture Proportions.

Materials	PCC	Water	Silica Sand	SP	VMA	Accelerator	CaCO₃
Proportion	1	0.334	1.5	0.004	0.003	0.04	0.2

Note: all numbers are mass ratios of PCC weight

Table 3. Reinforcing Material Properties

Diameter (mm)	Yield Strength (MPa)	Ultimate Strength (MPa)	Elongation (%)	Tensile Elasticity Modulus (GPa)
6	449	499	2.00	180
8	434	647	9.89	206
10	401	452	4.12	211

Figure 3. Stress-strain Relationships of Steel Bar Cut from Wiremesh: (a) Diameter 6 mm, (b) Diameter 8 mm, and (c) Diameter 10 mm

Specimen Production

The 3D printed concrete beams were produced using 3D printing concrete machine at Structural Engineering Laboratory of Petra Christian University, Indonesia (see Figure 4). The 3D printed concrete beams were printed with double filaments of 50 mm width and 20 mm layer height while keeping the printing speed at 2 cm/s. A custom vibration-based extruder was used to extrude concrete material at constant flowing rate. The fresh concrete was manually placed towards the extruder where an active vibrator ensured the homogenous of the concrete. The machine utilizes CNC machine concept in which the movement of the machine is done using G-Code which is executed by an operator. The machine was run in manual control mode as both the reinforcement and concrete mixture were placed manually. For all specimens, the reinforcement was added manually after the first layer (20 mm). Once printed, the specimen was cut to the desired length (550 mm) to ensure smooth surface for the grouting process. Table 4 gives an overview of the specimens' properties. The 3D printed specimens did not match the exact same dimensions as the conventional ones, and therefore the reinforcement ratio (ρ_{actual}) are slightly varied and the real dimensions were used for the analysis. Figure 5 shows the printing path of the machine in which the concrete was printed parallel to the longitudinal reinforcement. When needed, SikaGrout® 215 was used to make mortar beds in order to level the spreader beam on 3D printed specimens. The conventionally cast concrete beams were produced with the same mixture using wooden formwork. Before testing, all specimen surfaces were painted white for easier cracks identification. Figure 6 visualizes a typical 3D printed concrete beam specimen which was tested on this research.

Figure 4. 3D Printing Concrete Machine at Structural Engineering Laboratory of Petra Christian University, Indonesia

Table 4. Specimen Properties

Type	Specimen ID	b_w (mm)	h (mm)	ρ_{actual}	f'_c (MPa)
Conventional	PC-0	100	100	0	43.75
	PC-0.37	100	100	0.0037	45.33
	PC-0.73	100	100	0.0073	41.89
	PC-1.05	100	100	0.0105	41.11
	PC-1.32	100	100	0.0132	42.24
3D Printed	3D-0	105	95	0	24.86
	3D-0.37	120	95	0.0034	23.00
	3D-0.73	110	111	0.0058	24.41
	3D-1.05	115	95	0.0093	27.00
	3D-1.32	115	115	0.0105	22.63

Figure 5. Printing Path to Produce 3D Printed Concrete Beam Specimens
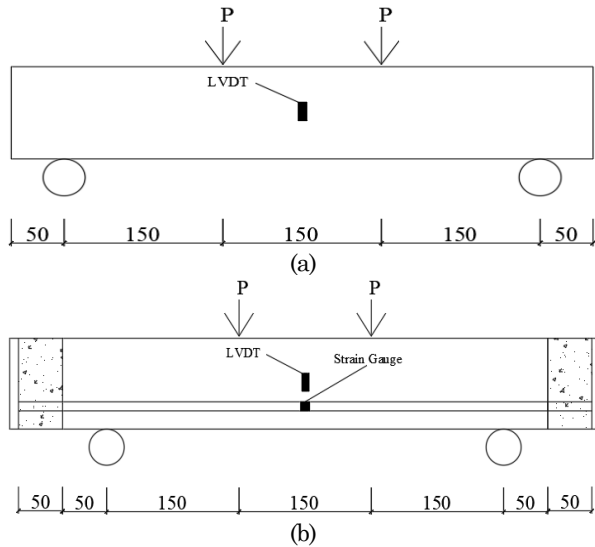

Figure 6. A Typical 3D Printed Concrete Beam Specimen

Three cube specimens were produced for testing the compressive strength of the concrete. For the conventionally cast beams, the compressive strength specimens were created by using 50 x 50 x 50 mm molds whereas for the 3D printed beams, the cubes were created by printing a single filament with 3 layers (60 mm thick) of concrete. The filament was then manually cut when the concrete was still in the fresh stage. All the compressive strength specimens were tested on the same day as the beam specimens.

Measuring Instrumentations and Testing Procedure

Four-point flexural test was used to test all beam specimens. Mid-span displacement of each beam specimen was measured using linear variable displacement transformer (LVDT). Strain gauges were installed at the middle of longitudinal reinforcements to obtain the strain during testing. Complete setups are shown in Figure 7.

The monotonic loading was applied using a hydraulic cylinder which was connected to a load cell to monitor the load. A spreader beam was used to transfer the load to the specimens. A data logger was used to record the load, mid-span deflection, and steel strain during testing. The test setup is shown in Figure 8.

Figure 7. Test Setup and Measuring Instruments; (a) Beam Without Reinforcement and (b) Beam with Reinforcement
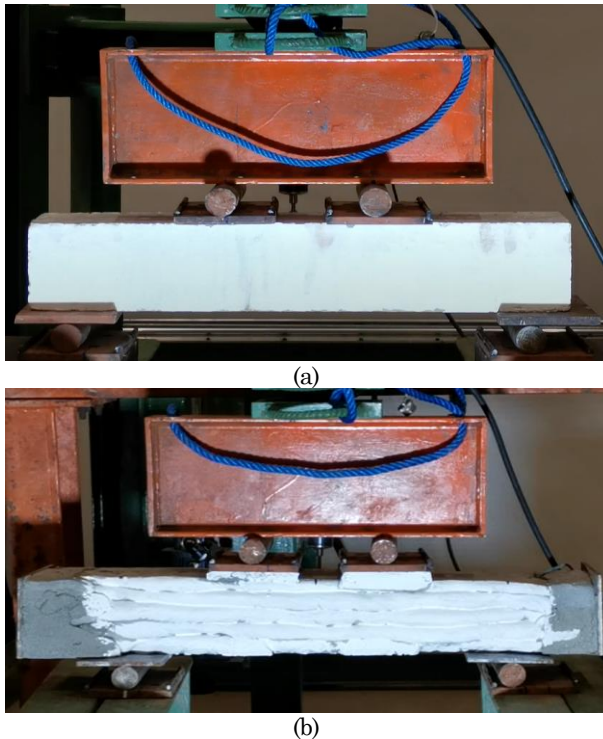
Figure 8. Typical Test Setup; (a) Conventional Concrete Beam and (b) 3D Printed Concrete Beam
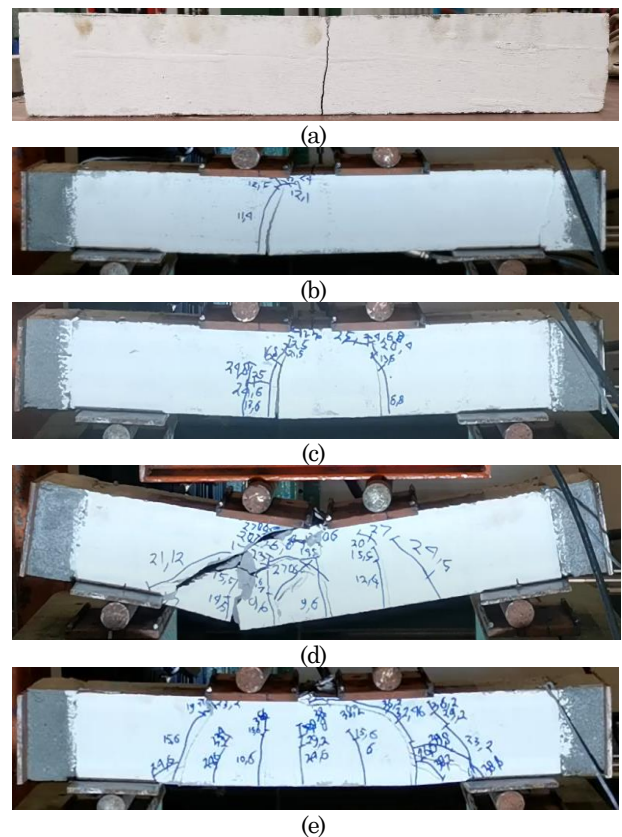
Experimental Results and Discussions

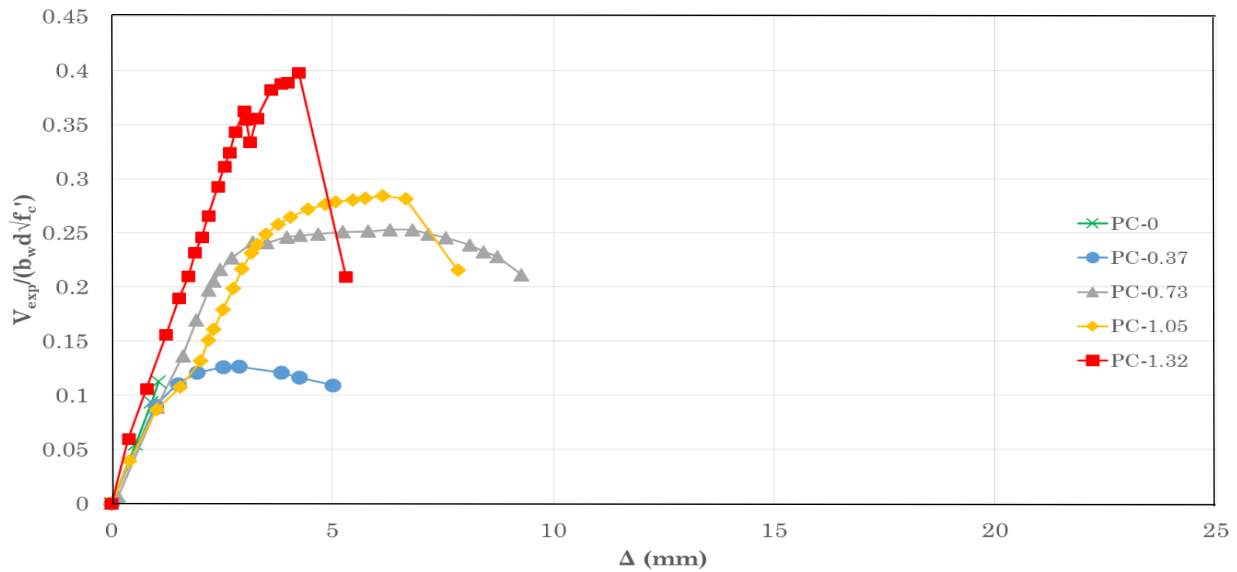### Conventional Concrete Specimens

The crack patterns and load-displacement relationships of conventional concrete specimens are shown in Figures 9 and 10, respectively. The numbers written on the side of the cracks reflect the amount of point load (2P) from the hydraulic cylinder which was applied on the spreader beam. Maximum internal shear force that occurred on the beam (V_{exp}) is normalized by beam's effective area and square root of concrete compressive strength to equally compare the performance of the specimens as shown in Table 5.

The test results show that specimens failed in flexural mode started with linear uncracked phase followed by the formation of one or two bending cracks which then widen until failure of the specimens. Only specimen PC-0.73 formed new bending cracks when it almost reached its maximum capacity which then resulted in higher ductility than other specimens failed in flexural mode. Specimens failed in shear mode behaved similarly only in the linear uncracked phase. After the uncracked phase, specimen PC-1.05 formed bending cracks followed with diagonal tension cracks after reaching its maximum capacity and ultimately failed in shear. For specimen PC-1.32, after the uncracked phase, the beam formed bending cracks together with diagonal tension cracks and after reaching its maximum capacity the beam failed in brittle manner.

Figure 10 and Table 5 explicitly display the effect of longitudinal reinforcement on the performance of conventional concrete beams. Higher ratio of longitudinal reinforcement yields higher capacity of conventional concrete beams for specimens failing in both flexural and shear mode. Furthermore, it can be seen from Figure 10 that specimens failing in flexural have more ductility as compared to specimens failing in shear. The load dropped gradually after reaching its peak for specimens failing in flexural whereas for specimens failing in shear, there was a sudden drop in load after reaching its maximum point.

Figure 9. Crack Patterns of Each Specimen; (a) PC-0, (b) PC-0.37, (c) PC-0.73, (d) PC-1.05, and (e) PC-1.32

Figure 10. Load-displacement Relationships of Conventional Concrete Specimens

Table 5. Experimental Results of Conventional Concrete Specimens

Specimen ID	f_c' (MPa)	ρ_{actual}	V_{exp} (kN)	Δ_{max} (mm)	$V_{exp}/(b_wd\sqrt{f_c'})$	Failure Mode
PC-0	43.75	0.0000	5.60	1.07	0.11	Flexural
PC-0.37	45.33	0.0037	6.57	5.00	0.13	Flexural
PC-0.73	41.89	0.0073	12.60	9.28	0.25	Flexural
PC-1.05	41.11	0.0105	13.67	7.84	0.28	Shear
PC-1.32	42.24	0.0132	19.90	5.31	0.40	Shear

3D Printed Concrete Specimens

Crack patterns of 3D printed concrete beams are displayed in Figure 11, with numerical notes indicating the amount of point load applied on the spreader beam at the formation of cracks. Specimens 3D-0, 3D-0.37, and 3D-1.05 failed similar to conventional concrete specimens failing in flexure in which the bending cracks developed and widened until failure of the specimens without spalling of concrete layers. However, it was not the case for specimen 3D-0.73 which failed differently than the others. After occurrence of some bending cracks, there was a horizontal interlayer crack at the bottom filament which ultimately caused spalling of the filament and led to a drop in the beam's capacity. Similar crack patterns were also observed in specimen 3D-1.32 in which after propagation of some bending and diagonal shear cracks, there were horizontal interlayer cracks that ultimately caused spalling of concrete filaments.

Figure 12 shows the load-displacement relationships of 3D printed concrete specimens. From the figure, it can be concluded that higher longitudinal reinforcement ratio also gives higher capacity for 3D printed concrete beams. It can also be concluded that in most cases, the behavior of 3D printed concrete beams are similar to those conventional concrete specimens.


(a)

(b)

(c)

(d)

(e)
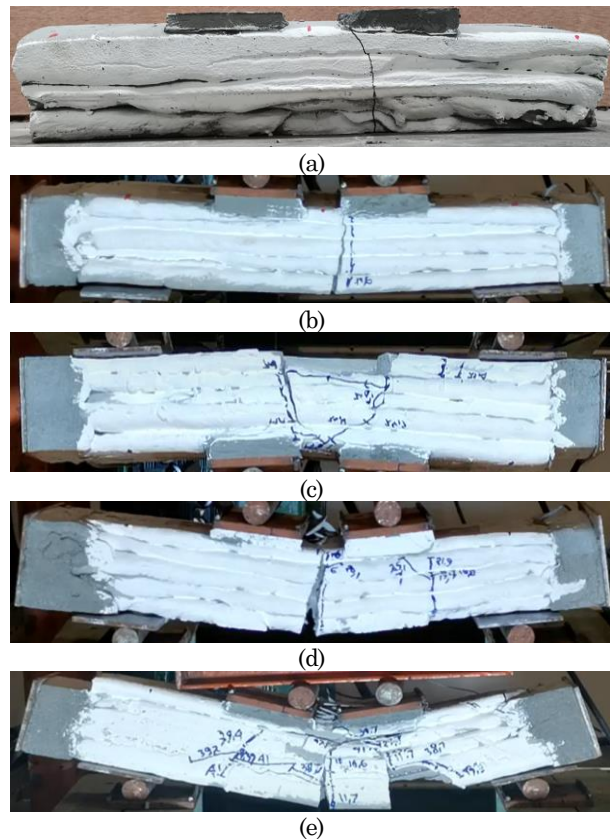
Figure 11. Crack Patterns of Each Specimen; (a) 3D-0, (b) 3D-0.37, (c) 3D-0.73, (d) 3D-1.05, and (e) 3D-1.32

Specimens failing in flexural exhibit higher ductility before failure while specimen failing in shear dropped its capacity after reaching maximum load. It is worth noting that there was a possibility of slippage in specimen 3D-0.37, in which when bending cracks were formed and the specimen reached its maximum capacity, the load dropped significantly. However, when the loading was continued, the beam's capacity could increase again before it failed in ductile manner by widening of bending cracks. Further investigation after testing revealed that there were macroscopic voids between steel bar and concrete filaments as shown in Figure 13. This might lead to less bond between steel bar and concrete filaments which caused the slippage. Details of the experimental results are shown in Table 6.

Comparison with ACI 318-14 Provisions

In this section, ACI 318-14 [14] methods are used to predict the strengths of both conventional and 3D printed concrete beams. Since there is no guideline for calculating the capacity of 3D printed concrete beams, conventional reinforced concrete methods are used to calculate the strength of 3D printed concrete beams. Experimental results from this study (V_{exp}) are compared with calculated capacities from ACI code (V_n). The comparisons are tabulated in Table 7 and Table 8 for conventional concrete beams and 3D printed concrete beams, respectively. Furthermore, the predicted failure modes from ACI code are also compared with failure modes obtained from the experiment.
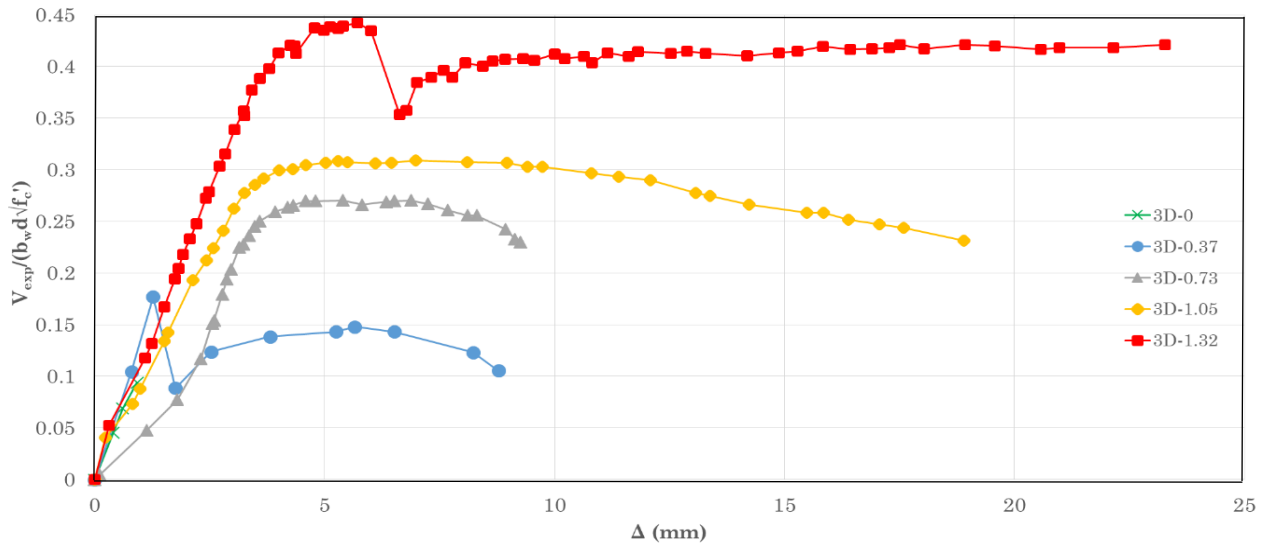
Figure 12. Load-displacement Relationships of 3D Printed Concrete Specimens

Figure 13. Macroscopic Voids between Steel Bar and 3D Printed Concrete Filaments Found in Specimen 3D-0.37

Table 6. Experimental Results of 3D Printed Concrete Specimens

Specimen ID	f_c' (MPa)	ρ_{actual}	V_{exp} (kN)	Δ_{max} (mm)	$V_{exp}/(b_w d\sqrt{f_c'})$	Failure Mode
3D-0	24.86	0.0000	3.50	0.93	0.09	Flexural
3D-0.37	23.00	0.0033	7.33	8.78	0.18	Flexural
3D-0.73	24.41	0.0058	12.93	9.14	0.27	Flexural
3D-1.05	27.00	0.0098	12.93	18.90	0.31	Flexural
3D-1.32	22.63	0.0096	22.03	23.27	0.44	Shear

Table 7. Failure Mode and Capacity Comparison of Conventional Concrete Specimens

Specimen ID	Failure Mode		V_{exp}/V_n
	Experimental	Analytical	
PC-0	Flexural	Flexural	1.23
PC-0.37	Flexural	Flexural	1.03
PC-0.73	Flexural	Flexural	1.01
PC-1.05	Shear	Shear	0.98
PC-1.32	Shear	Shear	1.39

Table 8. Failure Mode and Capacity Comparison of 3D Printed Concrete Specimens

Specimen ID	Failure Mode		V_{exp}/V_n
	Experimental	Analytical	
3D-0	Flexural	Flexural	1.08
3D-0.37	Flexural	Flexural	1.25
3D-0.73	Flexural	Flexural	0.93
3D-1.05	Flexural	Shear	1.07
3D-1.32	Shear	Shear	1.53

From Table 7, it can be concluded that for conventional concrete, the predictions of the building code provision [14] seem to be conservative for specimens failing in shear while predictions for specimens failing in flexural have closer values to the experimental results. The failure modes of conventional concrete specimens are in agreement with the predictions from ACI code. From Table 8, it can be inferred that the conventional concrete methods are less accurate to predict the capacity of the 3D printed concrete specimens. This is shown by the V_{exp}/V_n values that are not close enough to 1.00 as compared to conventional concrete specimens. Furthermore, for specimen 3D-1.05, the prediction of failure mode from the code does not match with the failure mode that occurred in the experiment. This implies that the actual shear strength of specimen 3D-1.05 is higher than its flexural strength and hence, instead of failing in shear as predicted by the code, the specimen failed in ductile flexural mode. Moreover, it can be seen for specimen 3D-1.32, which failed in shear, the V_{exp}/V_n value is 1.53. This means that ACI code underestimates the shear strength of 3D printed concrete specimens by some margins.

Conclusions

Ten conventional and 3D printed concrete beams were tested using third point loading to study their behavior on flexural and shear stresses using various longitudinal reinforcement ratios. From the experimental results, the following conclusions were made:
1. Higher ratio of longitudinal reinforcement yields higher capacity of both conventional concrete beams and 3D printed concrete beams failing in flexural and shear. This is in agreement with building code provisions [14] for calculating the strength of reinforced concrete beams.

2. The influence of printing layers on the crack patterns of 3D printed concrete specimens is significant. It was found that in some 3D printed concrete specimens, there were horizontal interlayer cracks which caused spalling of concrete filaments and thus reduced the load carrying capacity of the beams.
3. 3D printed concrete beams were made by pouring layer-by-layer of concrete into the printing bed. This method of production might generate macroscopic voids between concrete filaments and steel bars that were put manually on the fresh filaments. Because of these voids, there was less bond between concrete filaments and steel bars which then resulted in slippage and sudden drop of the beam's capacity.
4. ACI 318-14 [14] predictions are reasonably accurate for conventional concrete specimens failing in flexural and are more conservative for those failing in shear. However, for 3D printed concrete specimens, the predictions are less accurate, especially for those failing in shear.

References

1. Schuldt, S.J., Jagoda, J.A., Hoisington, A.J., and Delorit, J.D., A Systematic Review and Analysis of the Viability of 3D-printed Construction in Remote Environments, *Automation in Construction*, 125, 2021, pp. 1-16.
2. Ma, G., Li, Z., Wang, L., and Bai, G., Micro-cable Reinforced Geopolymer Composite for Extrusion Based 3D Printing, *Materials Letters*, 235, 2019, pp. 144-147.
3. Le, T.T., Austin, S.A., Lim, S., Buswell R.A., Gibb, A.G.F., and Thorpe, T., Hardened Properties of High-performance Printing Concrete, *Cement and Concrete Research*, 42, 2012, pp. 558-566.
4. Wolfs, R.J.M., Bos, F.P., and Salet, T.A.M., Hardened Properties of 3D Printed Concrete: The Influence of Process Parameters on Interlayer Adhesion, *Cement and Concrete Research*, 119, 2019, pp. 132-140.
5. Rahul, A.V., Santhanam, M., Meena, H., and Ghani, Z., Mehanical Characterization of 3D Printable Concrete, *Construction and Building Materials*, 227, 2019, pp. 1-12.
6. Sanjayan, J.G., Nematollahi, B., Xia, M., and Marchment, T., Effect of Surface Moisture on Interlayer Strength of 3D Printed Concrete, *Construction and Building Materials, 172,* 2018, pp. 468-475.

7. Wang, H., Shao, J., Zhang, J., Zou, D., and Sun, X., Bond Shear Performances and Constitutive Model of Interfaces between Vertical and Horizontal Filaments of 3D Printed Concrete, *Construction and Building Materials*, 316, 2022, pp. 1-10.

8. Baz, B., Aouad, G., Leblond, P., Al-Mansouri, O., D'hondt, M., and Remond, S., Mechanical Assesment of Concrete–steel Bonding in 3D Printed Elements, *Construction and Building Materials*, 256, 2020, pp. 1-11.

9. Ding, T., Qin, F., Xiao, J., Chen, X., and Zuo, Z., Experimental Study on the Bond Behaviour between Steel Bars and 3D Printed Concrete, *Journal of Building Engineering*, 49, 2022, pp. 1-15.

10. Sun, X., Ye, B., Lin, K., and Wang, H., Shear Performance of 3D Printed Concrete Reinforced with Flexible or Rigid Materials based on Direct Shear Test, *Journal of Building Engineering*, 48, 2022, pp. 1-12.

11. Al-Chaar, G.K., Stynoski, P.B., and Banko, M.L., Structural Behavior of Layer-printed Reinforced Concrete Beams, *The Open Construction and Building Technology Journal*, 12, 2018, pp. 375-378.

12. Asprone, D., Auricchio, F., Menna, C., and Mercuri, V., 3D Printing of Reinforced Concrete Elements: Technology and Design Approach, *Construction and Building Materials*, 165, 2018, pp. 218-231.

13. Gebhard, L., Mata-Falcón, J., Anton, A., Dillenburger, B., and Kaufmann, W., Structural Behavior of 3D Printed Concrete Beams with Various Reinforcement Strategies, *Engineering Structures*, 240, 2021, pp. 1-14.

14. ACI 318-14, *Building Code Requirements for Structural Concrete*, American Concrete Institute, 2014.